http://dx.doi.org/10.14500/aro.11157

A Miniaturized wide Stopband Low-pass Filter using T and Modified L Shapes Resonators

Mani D. Fadaee, Farzin Shama, Mohammad S. Feali and Maryam S. Gilan

Department of Electrical Engineering, Kermanshah Branch, Islamic Azad University, Kermanshah, Iran

***Abstract*—A new structure of microstrip-based low-pass filter with wide stopband and sharp roll-off is introduced, in this paper. In the proposed topology, resonators with T and modified L Shapes have been used. To improve the suppression factor and relative stopband bandwidth, the second resonator has been added to the first resonator. The designed filter has been fabricated on a 20 mm thickness RO4003 substrate, which has a loss tangent of 0.0021 and a relative dielectric constant equal to 3.38. All parameters including roll of rate, stopband, bandwidth, return loss, insertion loss, and figure of merit have significant coefficients. Simulation has been ran using advanced design system software. The 3dB cutoff frequency is appropriate. The value of the insertion loss parameter is <0.1 dB and the S_{11} parameter is −22 dB at this point. The stopband is extended from 2.42 up to 24 GHz, which shows an ultra-stopband. The results of the simulation and experiment are almost similar, which indicates a proper performance of the designed structure.**

***Index Terms*—Low-pass filter, L-shaped, Microstrip, Resonator, Sharp roll off, T-shaped.**

I. Introduction

Microstrip filters are one of the main components of telecommunication systems because, unlike passive and active circuits, they are much smaller in size and cost less. In recent years, researchers have developed microstrip filters using related structures. Each of these structures has strengths and weaknesses that can be combined to achieve a new structure with the improvement of all parameters (Chen, Li, and Chu, 2017; Du, Yang, Zhang, H., and Zhu, 2014; Imani, Shama, Alirezapoori, and Ekhteraei, 2018; Kolahi and Shama, 2018; Kumar and Parihar, 2016; Rekha, Abdulla, Jasmine, and Anu, 2020; Shama, Hayati, and Ekhteraei, 2018; Wang, Xu, Zhao, Guo, and Wu, 2010; Wei, Chen, and Shi, 2012).

In the design of microstrip low-pass filters (LPF), the small size of the filter always plays an important role. Semicircular structures in the filter design reduce the size of the circuit and follow the above rule. However, the suggested structures have a problem such as inappropriate transition bands in the passband and very low stopband bandwidth (Hiedari and Shama, 2018).

Using a symmetrical parallel-coupled line structure, a new microstrip LPF has been designed (Jiang, et al. 2017). This structure has very low insertion loss, which is the biggest advantage of the introduced filter. In the stopband, the value of suppression is not enough, which leads to a quality reduction of the LPF (Jiang, et al. 2017).

Defected ground structure (DGS) is used to design an ultra-wide stopband bandwidth. Although the proposed structure produces an appropriate stopband bandwidth, the proposed double-layer architectural factor reduces the figure of merit. One of the most important parameters in the design of microstrip LPF is the appropriateness of the filter dimensions (Bhat, et al., 2018).

As mentioned, various structures including T-shaped, semicircular shapes, symmetric parallel coupled lines, and DGS have been proposed. Each of the above structures affected the value such as sharpness in the transition band, stopband bandwidth, return loss, insertion loss, and dimensions. However, each of these structures may improve one of the filter response properties, so achieving a response with various suitable properties may not be possible with just one structure.

In this research, a microstrip LPF with a T-shaped resonator and modified L-shaped resonator is simulated, fabricated, and measured. All response factors such as Roll of rate, stopband bandwidth, return loss, insertion loss, and figure of merit have significant values. All simulations are performed using advanced design system software. Using a RO4003 substrate with 20 mm thickness the proposed filter was implemented. RO4003 has a loss tangent of 0.0021 and a dielectric constant equal to 3.38.

II. Main Resonator

The proposed filter was designed using a T-shaped resonator. The suggested resonator has a good response with appropriate sharpness. The cutoff frequency is also appropriate. Calculated dimensions for the proposed resonator are: L_1 = 7.2 mm, L_2 = 8 mm, L_3 = 7.3 mm, L_4 = 3 mm, W_1 = 5 mm, W_2 = 6.85 mm, W_3 = 3.15 mm, W_4 = 1.18 mm, and T_1 = 0.1 mm and these dimensions are calculated using base resonators and then optimized (Blue arrows as the length, Green arrows as the width, and red arrows are considered as the Thickness). (Fig. 1a) shows the resonator structure.

ARO-The Scientific Journal of Koya University
Vol. XI, No. 1 (2023), Article ID: ARO.11157, 5 pages
DOI: 10.14500/aro.11157
Received 12 February 2023; Accepted 27 April 2023
Regular research paper: Published: 18 May 2023
Corresponding author's e-mail: f.shama@aut.ac.ir

The proposed resonator frequency response from the simulation is shown in (Fig. 1b). The proposed resonator was able to create strong transmission zero at 2.41GHz. The measured value of transmission zero is −48 dB. By changing the value of L3, you can shift the cutoff frequency with transmission zero. However, it increases the insertion loss. The effect of changing parameter L3 is shown in Fig. 1.

The extracted equivalent circuit is depicted in Figs. 2 and 3. Methods discussed in (Hong and Lancaster, 2004; Pozar, 2011) can be used for extracting the values of parameters. (Fig. 2a) shows a low-impedance and high-impedance lossless line, in which both ends are terminated by low impedance-lines, which could also be introduced by a π-equivalent circuit, as shown in (Fig. 2b).

Inductors and capacitors will be obtained from the following equations:

$$L_S = \frac{1}{\omega} * z_S * sinsin\left(\frac{2\pi}{\lambda_g} l\right) \quad (1)$$

$$C_S = \frac{1}{\omega} * \frac{1}{Z_S} * tan(\frac{\pi}{\lambda_g} l) \quad (2)$$

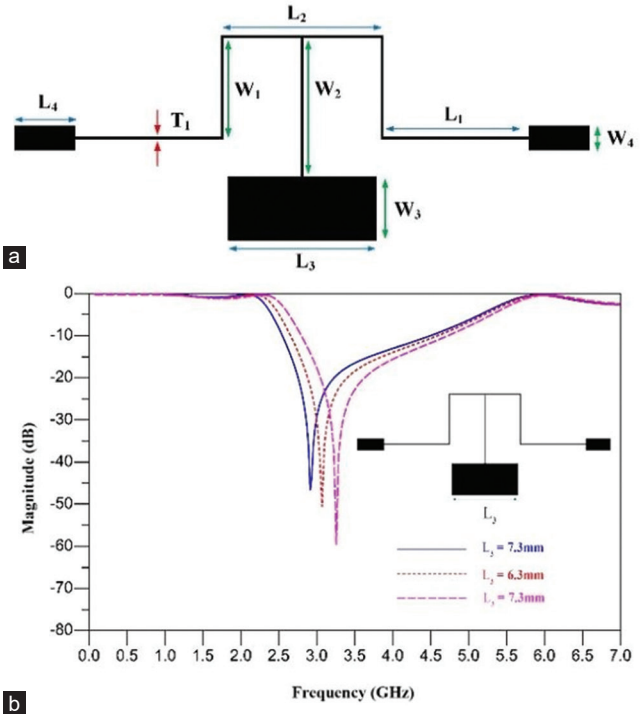

Fig. 1. (a) T-shaped resonator and (b) T-shaped resonator frequency response.

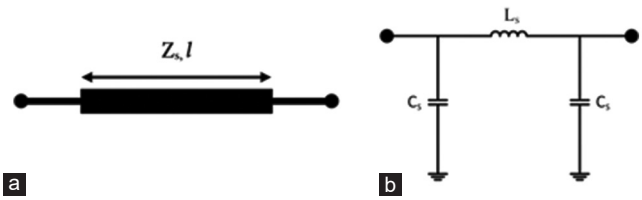

Fig. 2. (a) Low/high-impedance line and (b) LC model for a line.

In these equations, z_s, l, and λ_g represent the line characteristic impedance, the line length, and the guided wavelength, respectively. Open-end formulas were introduced in (Hong and Lancaster, 2004). In addition, (Fig. 3a and b) shows the structure and equivalent circuit.

For the T-shaped resonator, the LC equivalent circuit was extracted, considering the models introduced in Figs. 2 and 3. Equations 1 and 2 are used to calculate the values of the inductors and capacitors, respectively. (Fig. 4a) depicted the extracted LC equivalent circuit. Table I also shows the values of inductors and capacitors.

The transformation function can be expressed based on the proposed resonator equivalent LC circuit, represented in the following. By changing the parameters in the transformation function, the cutoff frequency can be shifted. The effect of this shifting appears on the insertion loss and increases it.

$$\frac{v_o}{v_i} = \frac{\begin{array}{c}A\times((B\times D\times c1S+E+L1S+L2S+2\times L4S+2\times L5S)\\ \times c2S+F\times(R+L3S)\times c2S+2+G)\end{array}}{(H\times((B\times M\times c1S+N+O)\times c3S+P)\times U)} \quad (3)$$

Fig. 3. (a) The open-end structure and (b) equivalent circuit for LC.

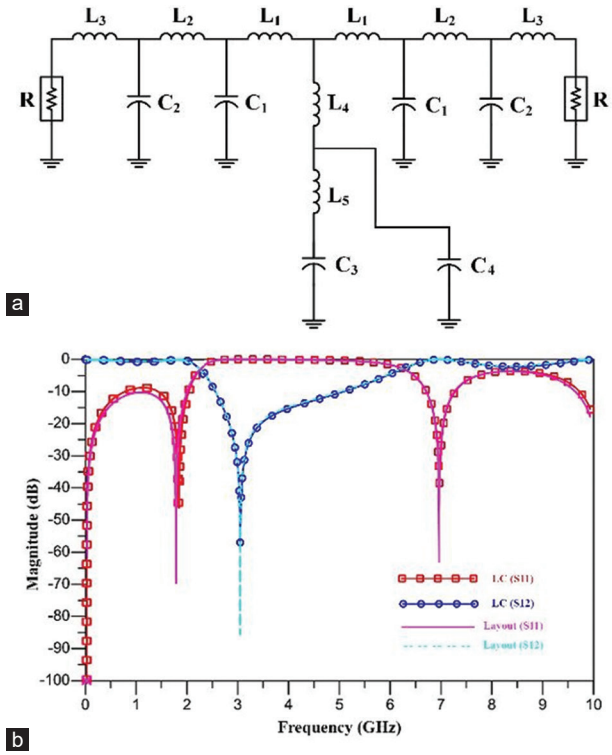

Fig. 4. (a) Resonator LC model and (b) frequency response diagram of the main resonator and LC equivalent circuit.

http://dx.doi.org/10.14500/aro.11157

$$A = B\times L_1S\times c_1S+(L_1S+L_2S)\times(R+L_3S)\times c2S+R+L_1S+L_2S+L_3S) \quad (4)$$

$$B = (L_2S\times(R+L_3S)\times c_2S+R+L_2S+L_3S) \quad (5)$$

$$D = (L_5S\times(L_1S+2\times L_4S)\times c_4S+L_1S+2\times L_4S+2\times L_5S) \quad (6)$$

$$E = (R+L_3S)\times(L_5S\times(L_1S+L_2S+2\times L_4S)\times c_4S) \quad (7)$$

$$F = (L_5S\times(R+L_1S+L_2S+L_3S+2\times L4S)\times c4S+R+L_1S+L_2S+L_3S+2\times L4S+2\times L_5S)\times c_3S+(2+(L_1S+2\times L_4S)\times c_4S)\times B\times c_1S+(2+(L_1S+L_2S+2\times L_4S)\times c_4S) \quad (8)$$

$$G = (R+L_1S+ L_2S+ L_3S+2\times L_4S)\times c_4S) \quad (9)$$

$$H = B\times c_1S+1+(R+L_3S)\times c_2S \quad (10)$$

$$M = (L_5S\times(L_1S+L_4S)\times c_4S+L_1S+L_4S+L_5S) \quad (11)$$

$$N = (L_5S\times(L_1S+L_2S+L_4S)\times c4S+L_1S+L_2S+L_4S+L_5S)\times(R+ L_3S)\times c_2S \quad (12)$$

$$O = L_5S\times(R+L_1S+L_2S+L_3S+L_4S)\times c_4S+R+L_1S+L_2S+L_3S+L_4S+L_5S \quad (13)$$

$$P = B\times(1+(L_1S+L_4S)\times c_4S)\times c_1S+(1+(L_1S+L_2S+L_4S)\times c_4S \quad (14)$$

$$U = (R+L_3S)\times c_2S+1+(R+L_1S+L_2S+L_3S+L_4S)\times c_4S \quad (15)$$

Where, R = 50Ω is the matching impedance. The transmission zero is generated at the frequency of 2.41 GHz with a magnitude of −48 dB. LC model and the designed layout are shown in (Fig. 4b). Good agreement between the LC and layout responses is obtained. However, this structure cannot be used alone. Because the suppression factor and relative stopband bandwidth (RSB) are not acceptable. To improve these parameters, the second resonator is inserted in the first resonator.

TABLE I
COMPUTED PARAMETERS FOR THE FIRST RESONATOR

Inductors	L_1	L_2	L_3	L_4	L_5
Inductances	2.1nH	4.7nH	2.4nH	3.8nH	0.8nH
Capacitors	C_1	C_2	C_3	C_4	-
Capacitances	0.3pF	0.2pF	0.001pF	2.2pF	-

III. Second Resonator

The proposed second resonator is designed using a modified L-shaped resonator. This resonator has very good dimensions and is designed to provide transmission zeros for increasing stopband bandwidth. Dimensions calculated for the designed resonator are as follows: T_2 = 0.1 mm, W_5 = 5.2 mm, and L_5 = 6.3 mm. The structure of the second resonator is shown in (Fig. 5a). The LC equivalent circuit is extracted based on Figs. 2 and 3 and depicted in (Fig. 5b). Capacitor and inductor values are calculated based on Equations 1 and 2 and are shown in Table II.

The frequency responses of the LC circuit and the proposed layout are shown in (Fig. 5c). The transmission zeros of the second resonator are generated at a frequency of 6.1 GHz with a magnitude of −178 dB. The modified L-shaped resonator has a good response in the stopband, but the sharpness is not suitable. To improve the above parameter, two resonators are combined.

IV. Combination of the First and Second Resonators

(Fig. 6a) shows the structure of the T-shaped and modified L-shaped resonators. The frequency response of the combination is just like a LPF, according to (Fig. 6b). The sharpness is very suitable, but the bandwidth is not a wide stopband. For improving the above parameter, the attenuator unit is used and added to the other resonator.

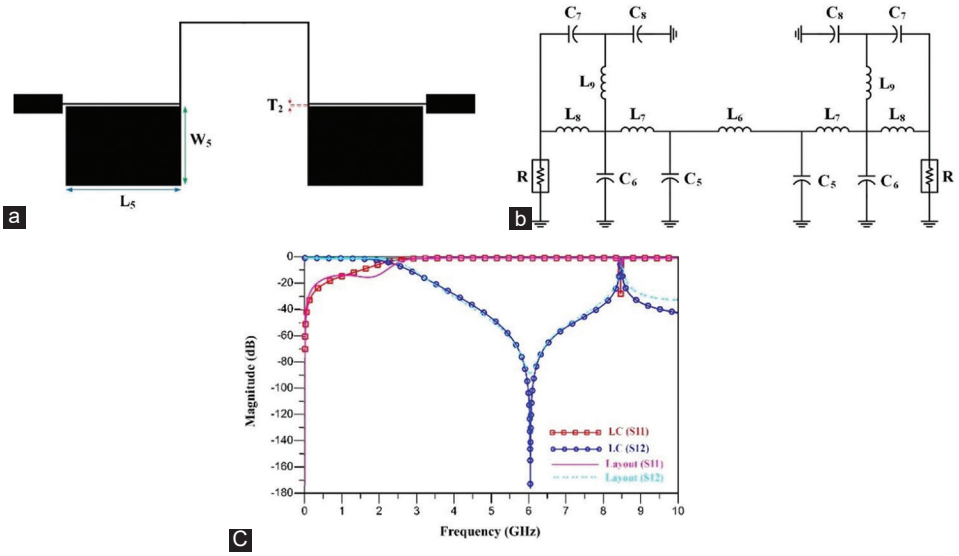

Fig. 5. (a) Structure of the second resonator, (b) LC model of the second resonator, and (c) simulated frequency response for the second resonator and LC model

TABLE II
COMPUTED PARAMETERS FOR THE SECOND RESONATOR

Inductors	L_6	L_7	L_8	L_9
Inductances	3.71nH	5.7nH	3.2nH	0.2nH
Capacitors	C_5	C_6	C_7	C_8
Capacitances	0.175pF	0.26pF	0.4pF	2.8pF

TABLE III
FILTER PARAMETERS CALCULATION TABLE

1	$\varepsilon = \frac{\alpha_{max} - \alpha_{min}}{F_s - F_c}$
2	$RSB = \frac{Stopband\ bandwidth}{Stopband\ center\ frequency}$
3	$SF = \frac{Rejectionlevelinstopband}{10}$
4	$NCS = \frac{PhysicalSize(Length * Width)}{\lambda_g^{\ 2}}$
5	$\lambda_g = \frac{300}{f_c \sqrt{\varepsilon_{re}}}$
6	$FOM = \frac{\varepsilon * RSB * SF}{NCS * AF}$

TABLE IV
COMPARISON CHART

Refs.	Roll-off	NCS (λg^2)	SF	AF	RSB	FOM
3	26	0.0180	2	1	1.34	3872
4	40.2	0.0117	1.5	1	1.60	8246
6	36.3	0.0062	1.5	2	1.32	11543
7	10.5	0.0324	2	1	1.46	949
8	81	0.0170	2	1	1.72	16400
9	100	0.0320	2	1	1.59	4968
10	44	0.0150	2	1	1.63	4723
11	45	0.0200	4	1	1.48	13320
12	103	0.0612	2	1	1.56	5269
13	81	0.0180	2.2	1	1.46	13140
14	56.7	0.0133	2	2	1.64	6983
15	35.4	0.0199	2	1	1.70	6051
16	62	0.0120	2	1	1.73	17876
17	100	0.0170	2	2	1.49	9030
18	148	0.0300	2	1	1.68	16576
Proposed filter	850	0.0420	2	1	1.64	66380

AF: Architectural factor, RSB: Relative stopband bandwidth, FOM: Figure of merit, NCS: Normalized circuit size

V. ATTENUATOR DESIGN

The modified L-shaped structure has been used in the design of the suppressor unit. The proposed suppressor unit and the frequency response of the final filter are depicted in (Fig. 7a and b), respectively. The dimensions of this suppressor unit are as follows:

According to the results presented in (Fig. 7b), all parameters have been significantly enhanced. The insertion loss parameter is <0.1dB and the return loss is −22 dB. The stopband is from 2.42GHz up to 24GHz. The roll-off rate is also very significant.

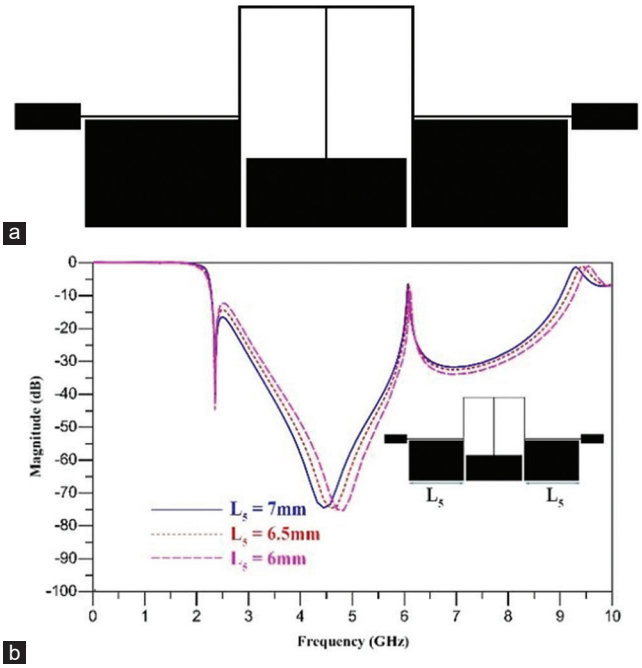

Fig. 6. (a) Structure of the main and second resonator and (b) the main and the second resonator comparison.

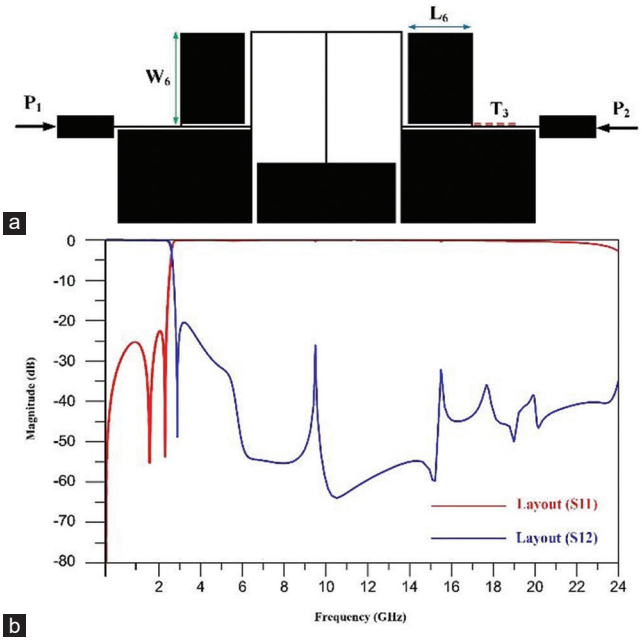

Fig. 7. (a) Structure of the proposed suppression unit with other resonators and (b) the final filter frequency response.

VI. RESULTS AND DISCUSSION

The filter is fabricated on a 20 mm thickness RO4003, (Fig. 8a). A comparison between the experimental and simulation results of the filter response is also depicted in (Fig. 8b). The filter dimension is 20.4 mm × 11 mm with an applicative cutoff at 2.4 GHz.

As seen in Table III, the most important factors in the filter response are defined and presented (Hayati, M., Abbasi, H., and Shama, F., 2014). It is clear from Table IV

http://dx.doi.org/10.14500/aro.11157

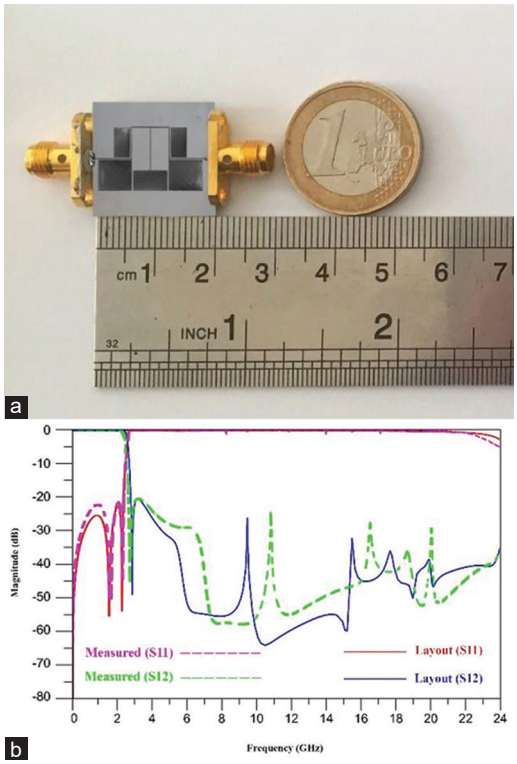

Fig. 8. (a) Fabricated circuit and (b) the final results for the fabricated filter.

that the designed LPF has the best roll-off rate between the mentioned works. In addition, with a high RSB, appropriate normalized circuit size (NCS), and good suppression factor (SF), it has a significant figure of merit (FOM) within these published works. Consequently, by considering these defined and conventional factors, besides having a smooth frequency response in the passband with minimum ripples (the insertion loss is significantly <0.1 dB, and the return loss is better than 20 dB in this band), the designed LPF is an appropriate candidate to attenuate the radiated n^{th} order harmonics on general wireless transmitters, which will be caused by non-linear blocks such as local oscillators, mixers, and power amplifiers. It is also ideal for reducing video transmitter interferences to nearby 2.4 GHz receivers and would be deposited between the transmitter and antenna.

VII. Conclusion

The steps of designing, simulating, fabricating, and measuring a microstrip LPF using a combination of T-shaped and modified L-shaped resonators are shown. The designed filter has a wide stopband from 2.42 GHz up to 24 GHz. The insertion loss is obtained <0.1dB and the return loss is −22 dB.

References

Bhat, U.R., Jha, K.R., and Singh, G., 2018. Wide stopband harmonic suppressed low-pass filter with novel DGS. *International Journal of RF and Microwave Computer-Aided Engineering*, 28(5), p.e21235.

Chen, F.C., Li, R.S., and Chu, Q.X., 2017. Ultra-wide stopband low-pass filter using multiple transmission zeros. *IEEE Access*, *5*, pp.6437-6443.

Du, Z., Yang, H., Zhang, H., and Zhu, M., 2014. Compact lowpass filter with high suppression level and wide stopband using stepped impedance m-shape units. *Microwave and Optical Technology Letters*, 56(12), pp.2947-2950.

Hayati, M., Abbasi, H., and Fathabadi, O.S., 2015. A novel microstrip lowpass filter with sharp roll-off and ultra-wide stopband using SICMRC. *International Journal of Electronics*, 102(9), pp.1475-1485.

Hayati, M., Abbasi, H., and Shama, F., 2014. Microstrip lowpass filter with ultrawide stopband and sharp roll-off. *Arabian Journal for Science and Engineerin*g, 39, pp.6249-6253.

Hayati, M., and Shama, F., 2017. A compact lowpass filter with ultra wide stopband using stepped impedance resonator. *Radioengineering*, 26(1), pp.269-274.

Hiedari, B., and Shama, F., 2018. A harmonics suppressed microstrip cell for integrated applications. *AEU-International Journal of Electronics and Communications*, 83, pp.519-22.

Hong, J.S.G., and Lancaster, M.J., 2004. *Microstrip Filters for RF/Microwave Applications*. John Wiley and Sons, United States.

Imani, M.A., Shama, F., Alirezapoori, M., and Ekhteraei, M., 2018. Miniaturized microstrip lowpass filter using cylindrical-shaped resonators for integrated applications. *Analog Integrated Circuits and Signal Processing*, 95, pp.223-229.

Jiang, S., and Xu, J., 2017. Compact microstrip lowpass filter with ultra-wide stopband based on dual-plane structure. *Electronics Letters*, 53(9) ,pp.607-609.

Jiang, Y., Wei, B., Heng, Y., Guo, X., Cao, B., and Jiang, L., 2017. Compact superconducting lowpass filter with wide stopband. *Electronics Letters*, 53(14), pp.931-933.

Kolahi, A., and Shama, F., 2018. Compact microstrip low pass filter with flat group-delay using triangle-shaped resonators. *AEU-International Journal of Electronics and Communications*, 83, pp.433-438.

Kumar, L., and Parihar, M.S., 2016. Compact hexagonal shape elliptical low pass filter with wide stop band. *IEEE Microwave and Wireless Components Letters*, 26(12), pp.978-980.

Pozar, D.M., 2011. *Microwave Engineering*. John wiley and Sons, United States.

Rekha, T.K., Abdulla, P., Jasmine, P.M., and Anu, A.R., 2020. Compact microstrip lowpass filter with high harmonics suppression using defected structures. *AEU-International Journal of Electronics and Communications*, 115, p.153032.

Shama, F., Hayati, M., and Ekhteraei, M., 2018. Compact microstrip lowpass filter using meandered unequal T-shaped resonator with ultra-wide rejection band. *AEU-International Journal of Electronics and Communications*, 85, pp.78-83.

Wang, J., Xu, L.J., Zhao, S., Guo, Y.X., and Wu, W., 2010. Compact quasi-elliptic microstrip lowpass filter with wide stopband. *Electronics Letters*, 46(20), pp.1384-1385.

Wei, F., Chen, L., and Shi, X.W., 2012. Compact lowpass filter based on coupled-line hairpin unit. *Electronics letters*, 48(7), p.1.